A Quick Sampling Method for Mapping Particle Distribution in Al-melt

M.Sc. Cong Li[1], M.Sc. Xiaoxin Zhang[1], Dr. -Ing. Mertol Gökelma[2], Dr. -Ing. Wolfram Stets[3], Prof. Dr.-Ing. Dr. h.c. Bernd Friedrich[1]

[1] RWTH Aachen University, IME – Process Metallurgy and Metal Recycling
Intzestraße 3
52056 Aachen, Germany

[2] Norwegian University of Science and Technology, Department of Materials Science and Engineering
Trondheim 7491, Norway

[3] Foseco Nederland BV
Pantheon 30
7521 PR Enschede, Netherlands

Keywords: melt sampling, particle distribution, sedimentation, agglomeration, aluminium melt, A356-SiC, MMC

Abstract

In order to produce high quality aluminium alloys with low non-metallic inclusion contents or high-strength aluminium matrix composites with well distributed particles, the distribution and concentration of solid particles in aluminium melts are considered fundamental enough to deserve practical interests. However, the high temperature and opacity of Al-melt have precluded simple observation techniques that have been utilized in aqueous systems. In the present study, a quick sampling method (QSM) for mapping spatial distribution of particles in Al-melt was developed based on the principle of conventional pipettes. The sampling procedure included a drawing operation of specimen melt and a subsequent quenching step. The ability of QSM to map particle distribution was demonstrated in a pre-prepared SiC particle-laden Al-Si melt. The evolution of particle volume fraction along the melt depth direction and agglomeration of particles were observed by applying QSM. Meanwhile, the weight loss (wt.-%) in QSM sampling operation was measured and compared with that in ideal cases.

1 Introduction

Particles, termed as reinforcement in aluminium matrix composites (AMC) [1] and inclusion in aluminium alloys [2], can strongly affect the mechanical properties of the desired products. During the production of both AMC and aluminium alloys, spatial distribution of particles within the melt

is intimately related with quality control and therefore is of both theoretical and technical interests [3, 4]. In stir casting process, a uniform spatial distribution of particles is a prerequisite of producing high quality AMC [5], whereas in melt purification, a decant melt with most of the detrimental particles e.g., Al_2O_3 segregated is favourable [6]. With an aim of closely controlling the quality of finished products, obtaining as much as possible the particle information with respect to size, concentration and distribution at various stages of melt treatment has always been desirable for the industry [7, 8]. However, opacity of Al-melt has precluded simple observation techniques employed in aqueous systems. Since years, several methods based on electrical or acoustical principle were developed to monitor particle in indirect ways [9, 10].

Liquid Metal Cleanliness Analyzer (LiMCA) is one of the most widely used setup which allows the aluminium producer to in-line and in-situ measure the concentration and size of inclusions within the melt. In this technique, 6 ml melt is forced to flow in and out of an orifice within the wall of a glass tube, during which the presence of non-conductive inclusions will lead to variation of electrical resistance between pre-immersed electrodes [11]. Recently, Gökelma et al. [12] and Badowski et al. [13] studied the sedimentation of inclusions in aluminium melt by measuring decrease of inclusion concentration at fixed positions under the melt surface using LiMCA. The sedimentation of inclusions taking place in the melt was clearly demonstrated by plotting variation of inclusion concentration over time. Based on identical principle of LiMCA, Hanumanth et al. [14] developed a simplified setup for acquiring information of volume fraction of particles in A356-SiC melt. The author placed three electrodes at different melt depths. By measuring the variation of electrical resistance at each depth in successive times, a time-dependent particle distribution map within the melt was deduced. Following the same experimental procedure, Irons et al. [15] studied the sedimentation of SiC particles whose size is in the range 10 – 15 μm in A356 melt. The final sediment volume fraction in the experiments was found to be 28 – 30 vol.-%. In this study, the Richardson and Zaki equation [16] that had been widely used to predict settling velocity of particles in suspensions was reviewed as well. Despite advantages of real time detection of particles in terms of concentration and size, in-line particle monitor techniques are incapable of providing knowledges with regard to type, shape as well as macroscopic (e.g., decant melt due to sedimentation) and microscopic (e.g., agglomeration of particles) spatial distribution of particles in the melt. The availability of gaining such information is drawing increasing attention given the continuous formation, transportation, sedimentation and agglomeration of inclusions within the melt [6, 7, 17]. From this respect, methods of melt sampling along with off-line specimen examination have their advantages.

Up to now, there are three available sampling methods capable of taking samples flexibly at different depths of aluminium melt:

1) “lollipop” sampler widely used in steel industry [18];
2) Liquid aluminium inclusion sampler (LAIS) [19];
3) Furnace sampling tool (FST) [20].

While operating, the lollipop and LAIS take samples by forcing the melt flow into a mould with the help of vacuum, whereas FST extracts the melt samples by utilizing the hydrostatic head. In indus-

trial-scale trials, functionality of the three methods has been proved. Nevertheless, if a complete map of inclusion within the melt is to be constructed by multiple sampling operations, either of any method has an inherent disadvantage: each sampling operation inevitably causes a melt turbulence, which will alter the distribution of inclusions in the remained melt. Furthermore, none of these methods can be used to study the agglomeration of particles, principally because the clusters are likely to be disturbed by melt flow during the course of sampling.

In the present work, a quick sampling method (QSM) was developed to macroscopically and microscopically map distribution of particles in a melt. Using this novel method, the sedimentation as well as agglomeration of particles were demonstrated in a SiC particle-laden Al-Si melt. Meanwhile, the wt.-% loss in QSM sampling operation under current experimental procedures was measured and compared with that in ideal cases.

2 Experimental Methodology

2.1 Quick Sampling Method (QSM)

With an aim of mapping particle distribution in the depth direction of a melt in one sampling action, the QSM should be able to enclose and withdraw the specimen melt which integrally carries information from bottom to the top of the research melt. In the meantime, the sampling operation ought to cause a minor disturbance of the enclosed specimen melt so as to save the particle distribution to the largest extent. Moreover, in order to avoid migration of particles induced by solidification, the method should also be designed so that the specimen melt can be quenched as soon as it was taken out.

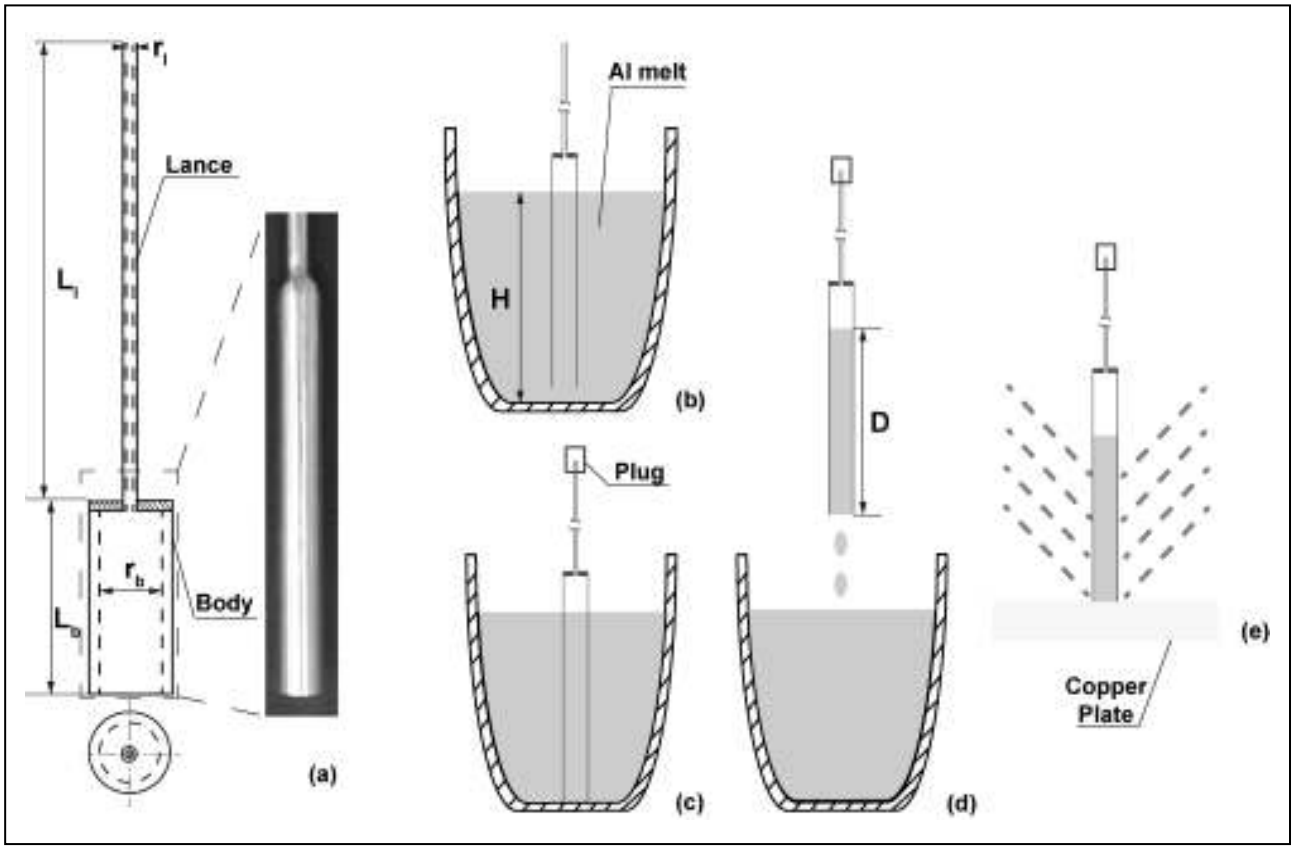

Figure 1: Schematic of sampler QSM design (a) and operation procedure (b) – (e).

A sampler with appearance of a conventional pipette was designed and made by stainless steel, consists of a body and a lance, as shown in Figure 1(a). In use, the pre-heated and boron nitride coated sampler body was firstly immersed very slowly into the melt in crucible until reaching the bottom (Figure 1(b)). Then, the lance was sealed with a plug at its top exit (Figure 1(c)). In the next step, the sampler body was drawn from the melt at a moderate speed, during which small amount of specimen melt dropped down and induced immediately a negative pressure inside the lance to withstand weight of the rest melt (Figure 1(d)). The quenching manner is schematically shown in Figure 1(e). A copper plate was used for supporting the sampler body and meantime quenched the contacted melt, shortly after which water was sprayed around the sampler body to quench the entire specimen melt.

Since QSM worked in principle by utilizing the pressure difference induced by dropping of the specimen melt, it is essential to clarify the amount of wt.-% loss. Consider an occasion occurs in Figure 1(c). At the moment the lance was sealed, the product of pressure P_1 and volume V_1 between specimen melt and top exit of the lance was given by ideal gas law:

$$p_1 V_1 = nRT \quad (1)$$

Where p_1 is atmosphere pressure, T is temperature, n is the number of moles of gas encapsulated between specimen melt and plug. R is ideal gas constant and V_1 is volume between specimen melt and plug calculated by:

$$V_1 = \pi L_l r_l^2 + \pi (L_b - H) r_b^2 \quad (2)$$

Where L_l and L_b are respective length of sampler lance and body, r_l and r_b are respective radius of sampler lance and body (Figure 1(a)). H is height of melt in crucible (Figure 1(b)). After the sampler body was drawn from the melt (Figure 1(d)), a new equilibrium was realized at the expense of losing specimen melt. The weight of remained specimen melt was withstood by pressure difference between p_1 and p_2:

$$\rho_{Al} g D = p_1 - p_2 \quad (3)$$

Where ρ_{Al} is density of the sampling melt and D is the length of remained specimen melt (Figure 1(d)). g is gravity acceleration and P_2 is the pressure between remained specimen melt and plug, given again by ideal gas law:

$$p_2 V_2 = nRT \quad (4)$$

Where V_2 is volume between remained specimen melt and plug determined by:

$$V_2 = \pi L_l r_l^2 + \pi (L_b - D) r_b^2 \quad (5)$$

Combined with Equation (1) through Equation (5), the wt.-% loss (WL) of specimen melt is given by:

$$WL = 1 - \frac{(p_1 r_b^2 + \rho_{Al} g r_l^2 L_l + \rho_{Al} g r_b^2 L_b) - \sqrt{(p_1 r_b^2 + \rho_{Al} g r_l^2 L_l + \rho_{Al} g r_b^2 L_b)^2 - 4 p_1 \rho_{Al} g r_b^4 H}}{2 \rho_{Al} g r_b^2} \quad (6)$$

Under current experimental procedures, the values of each parameter are specified in Table 1. By substituting the required values into Equation (6), the wt.-% loss is calculated to be 1.5%.

Table1: Constant Used for WL Calculation and Size Parameter of QSM Sampler

Parameter	p_1 [Pa]	ρ_{Al} [g/cm^3]	g (N/kg)	r_b [mm]	r_l [mm]	L_l [mm]	L_b [mm]	H [mm]
Value	99600	2.67	9.8	5	1.5	550	100	91

2.2 Experimental Procedure

Commercial pure aluminium (Al ≥ 99.7 wt.-%) supplied by Trimet Aluminium SE (Essen, Germany) and A356 – 17 vol.-% SiC composite supplied by OHM & HÄNER METALLWERK GmbH & Co. KG (Olpe, Germany) were used to prepare SiC particle-laden melt.

The melt preparation was carried out in a clay-graphite crucible with inner diameter of 85 mm and height of 150 mm, which was placed inside a Thermo-Star resistance-heated furnace. The furnace was covered with insulating lids and blankets with only two small opening left for stirrer, sampler and thermal couple. The stirrer was fabricated from graphite, connected with a steel shaft which was driven by a liftable motor. A K-type thermocouple covered by a protective alumina tube was used to monitor the melt temperature. A schematic illustration of the setup is presented in Figure 2.

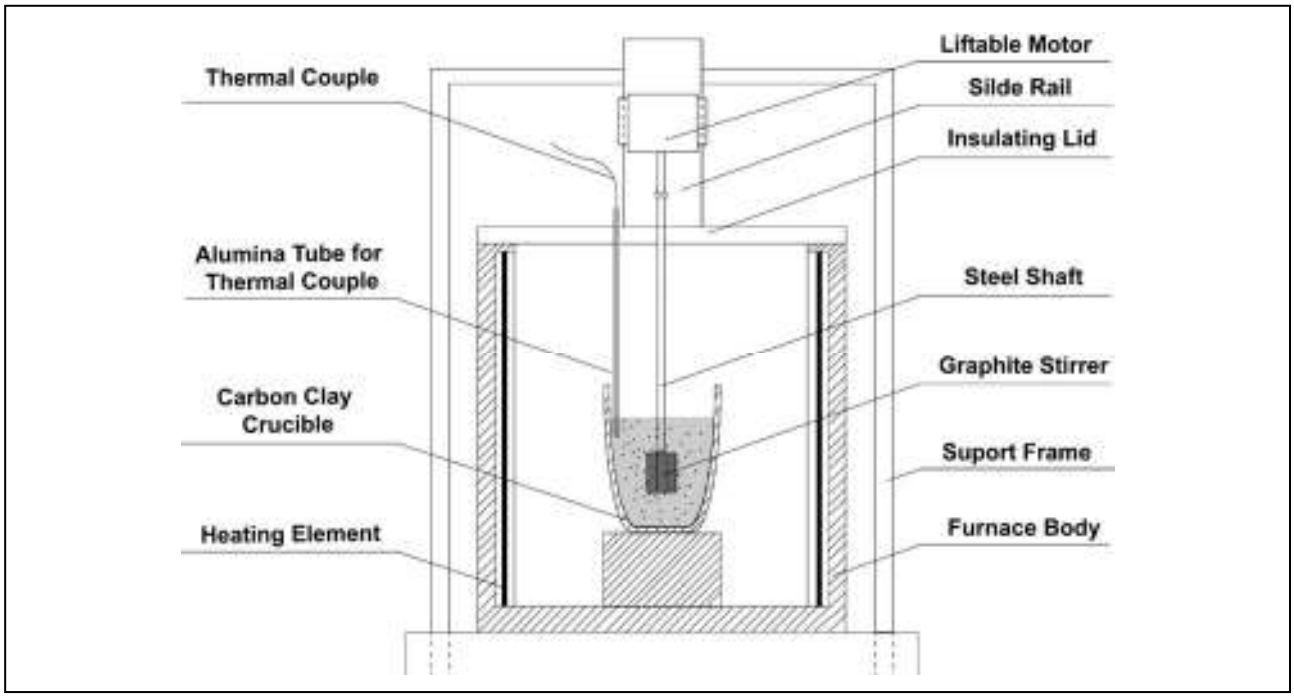

Figure 2: Schematic of experimental setup.

Initially, 884.2g of aluminium was charged into the crucible to produce a melt basis. When the melt reached 740°C, 216.8g A356-SiC composite was added into the melt in three steps. The melt was then held at 740°C for 30 min. Subsequently, it was stirred by a pre-heated stirrer at a speed of 400 rpm for 10 min. At the end of stirring, the stirrer was stopped and drawn from the melt and QSM was applied to take the first sample. Shortly after the first sample was taken out, the melt was stirred again. Then it was set at rest for 15 min before second sample was taken by QSM. The third and fourth samples were taken by the same procedure as the second one yet with the melt set at rest for 30 min and 45 min. Note that at each time in prior to sampling, the height of melt was measured by the stirrer positioned in advance with a known distance to the bottom of crucible. The stirring and dwell time for each sample before applying QSM is listed in Table 2.

Table 2: Stirring and Dwell Time for Each Sample

Sample	1st	2nd	3rd	4th
Stirring time [min]	10	10	10	10
Dwell time [min]	0	15	30	45

Samples were weighed and then cut in the long direction for the following polishing treatment. Surface of the section was prepared by successively grinding, lapping and polishing. The polishing was performed on chemical resistant cloth after lapping was finished with grade 2000 emery paper. After each step in above treatment of surface, the sample was thoroughly cleaned ultrasonically in anhydrous ethanol and dried in warm air.

2.3 Sample Characterization

The metallographic analysis of the samples was performed with a Keyence VHS-600 Optical Microscope. For each sample, more than 35 OM micrographs were successively taken along the long direction and combined side by side to present a complete picture of spatial distribution of SiC particles.

With an intent of studying sedimentation, distinction of particle volume fraction along the long direction was quantified with the help of a commercial software Image-Pro Plus 6.0 (MediaCybernetics, Inc., SilverSpring. MD). This software can automatically mark each particle / cluster in an input image and determine the corresponding area and diameter values. An example case is shown in Figure 3(a) – (c), where all particles in A356 – 17 vol.-% SiC were readily marked and their size distribution was given.

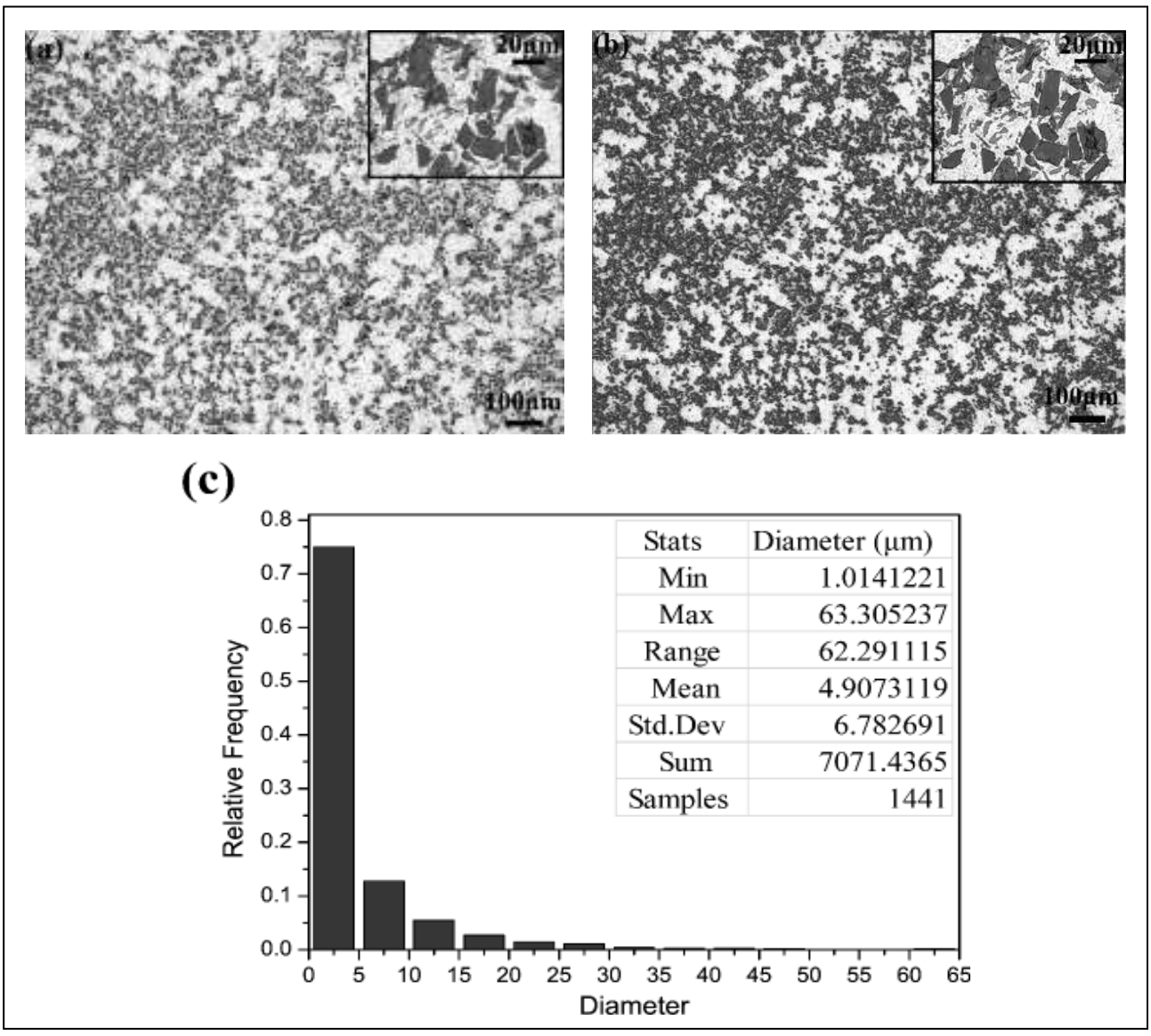

Figure 3: Identification of particles by using Image-Pro Plus 6.0: (a) OM micrograph taken from A356 – 17 vol.-% SiC; (b) contour of particles were identified; (c) Size distribution of identified particles.

Sedimentation was evaluated by characteristic particle volume fraction determined by:

$$RAA = \frac{P}{F} \tag{7}$$

Where P is the accumulated area of particles in a view field and F is the area of that view field. For each sample, the values of P and F were collected from more than 30 OM micrographs.

3 Results and Discussion

3.1 Wt.-% loss during sampling

In design of QSM, the wt.-% loss had been calculated in an ideal case to be 1.5 %. This value needs to be further verified or corrected in practical applications. In this section, the actual wt.-% loss (awl) during sampling operation will be determined by:

$$awl = w_s - w_m \tag{8}$$

Where w_s is weight of solidified sample (Figure 1(e)) and w_m is weight of specimen melt initially enclosed by sampler (Figure 1(c)) calculated by

$$w_m = r_b^2 H \rho_{Al} \tag{9}$$

Sections of the four samples taken by QSM are shown in Figure 4. For each sample, the melt height in crucible prior to sampling, length and weight of solidified cylinder sample and actual wt.-% loss is specified in Table 3.

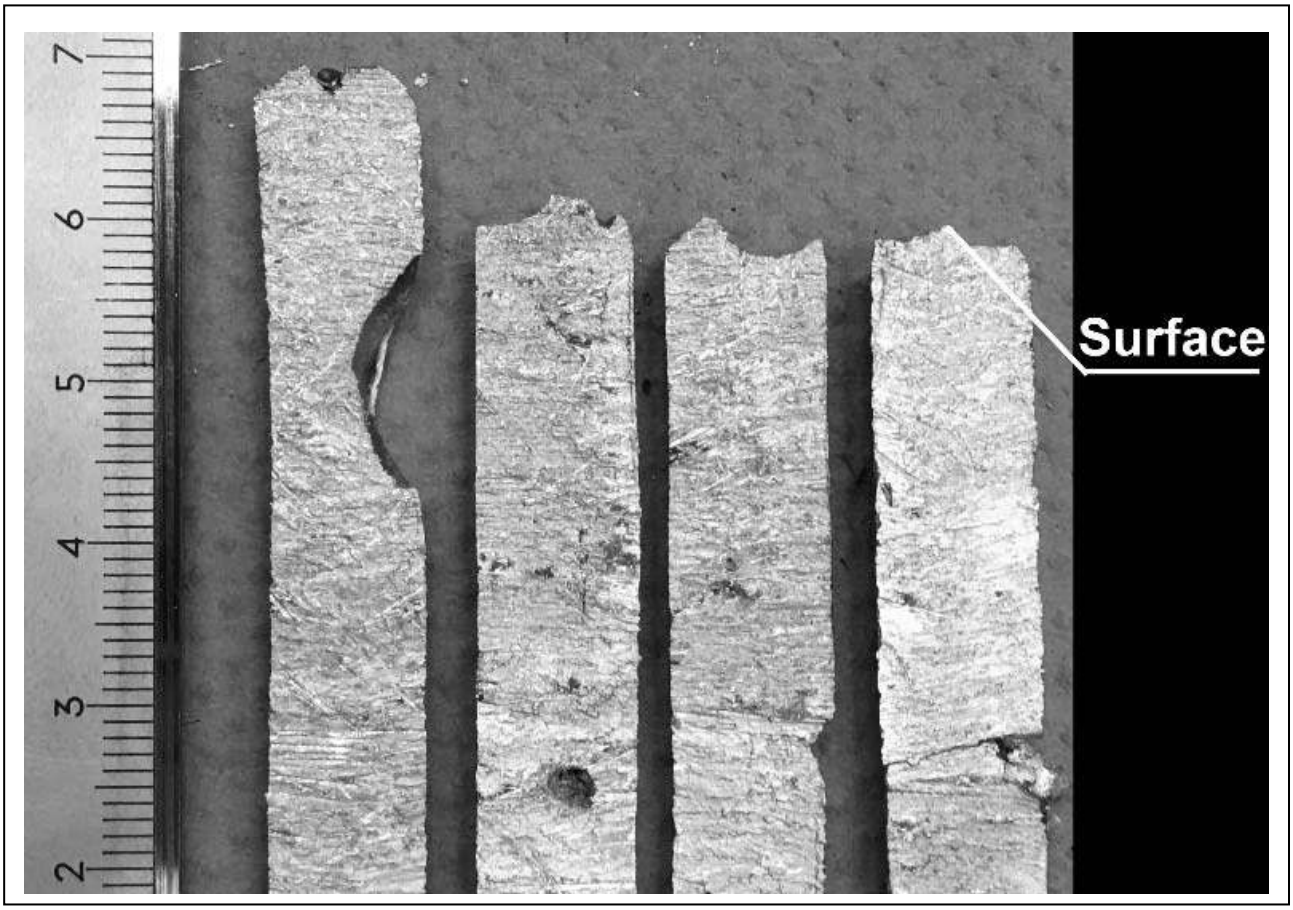

Figure 4: Section of the four samples taken from melt with 0 min, 15 min, 30 min and 45 min dwell time.

Table 3: Melt Height in Crucible Prior to Sampling, Length and Weight of Solidified Cylinder Sample and Actual wt.-% Loss

Sample	0 min	15 min	30 min	45 min
Melt height prior to sampling (mm)	91	88.5	87	86
Length of solidified sample (mm)	69	60	59	59
Weight of solidified sample (g)	15.5	14.8	14.4	13.4
Actual wt.-% loss	19	20	21.1	25.7

The wt.-% loss in both ideal and practical cases, plotted as a function of melt height in prior to sampling, is presented in Figure 5. It is illustrated that:

1) the actual weight loss ratio is around 10 times of that in ideal cases;
2) wt.-% loss in practical cases increased much more rapidly than in ideal cases with the decrease of melt height.

It is speculated the extra weight loss was due to high viscosity of the melt, which exerted a pull upon the specimen melt at the moment the sampler was drawn out of melt surface. In future works,

measures such as incorporating vacuum system into QSM will be tested in order to alleviate the weight loss problem.

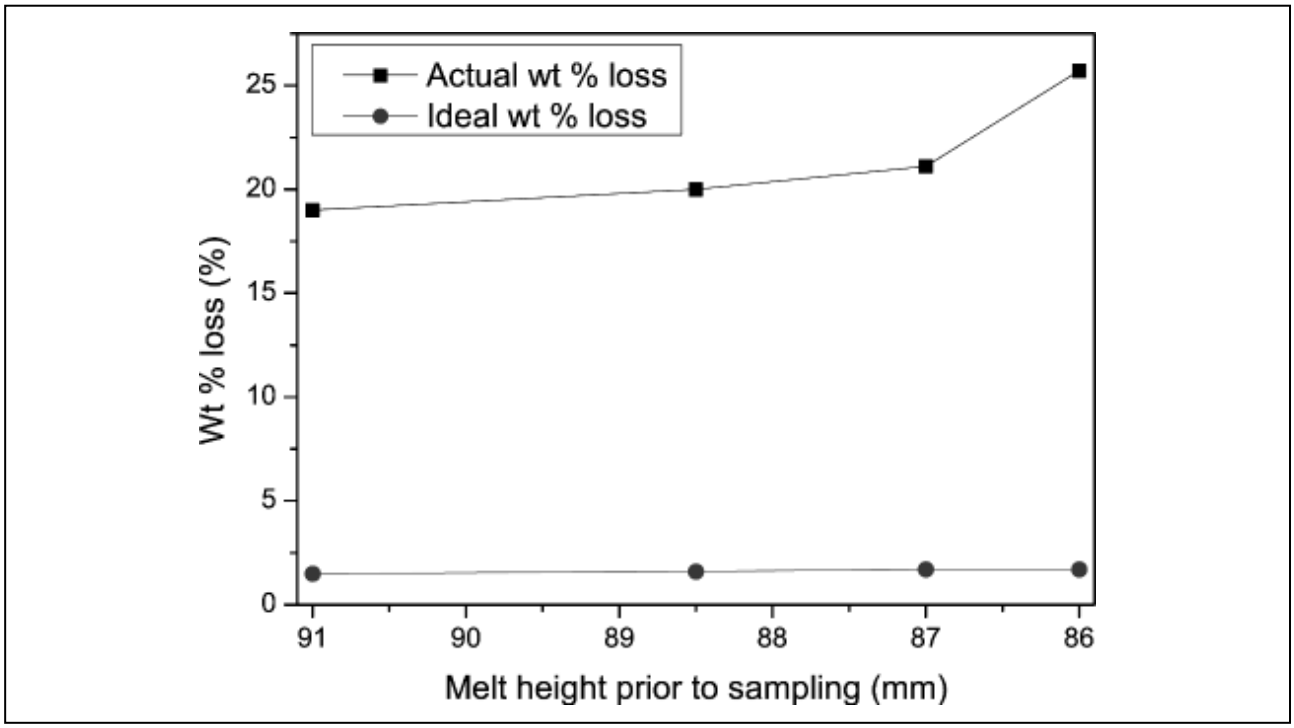

Figure 5: Variation of wt.-% loss in ideal and practical cases.

3.2 Sedimentation

Over the remainder part of this paper, we have unfortunately to focus on the remained specimen melt and hence all the melt mentioned hereinafter is specially referred to that with a depth (from top surface) less than 60 mm. In addition, for the sake of simplicity, the shrinkage of sample caused by solidification is ignored.

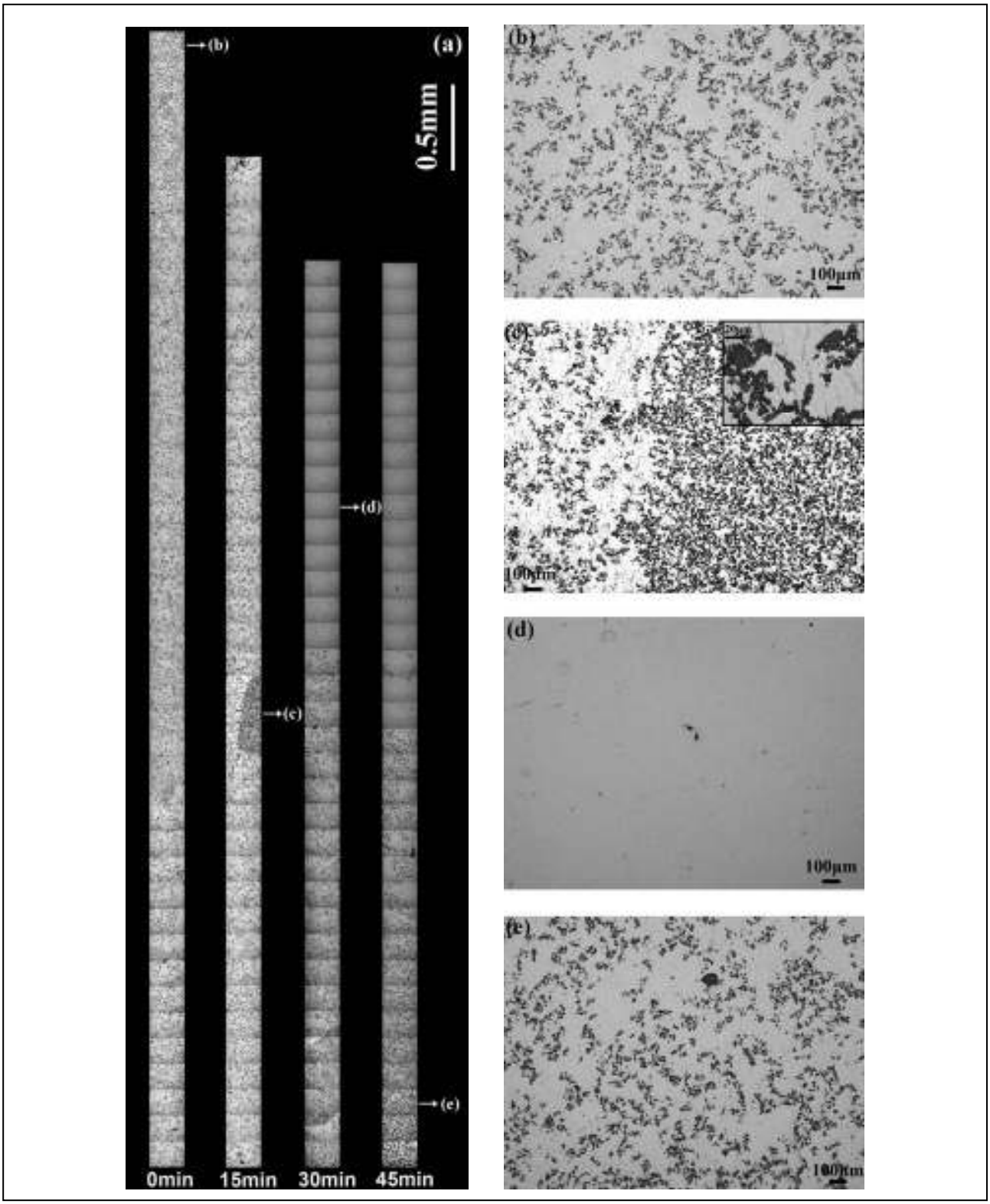

Figure 6: OM micrographs show the distribution of SiC particles along height direction in samples taken from the melt with 0 min, 15 min, 30 min and 45 min dwell time: (a) a complete view; (b) – (e) enlargement of four typical view fields. The insert in (c) is a close-up of the "aggregate".

Figure 6(a) presents completely the distribution of SiC particles along long direction in samples taken from melt with 0 min, 15 min, 30 min and 45 min dwell time. Enlargement of four typical view fields of Figure 6(a) are shown in Figure 6(b) – (e). At the end of melt stirring, particles were found to disperse uniformly in melt ("0 min" sample). Whereas in the case of 15 min dwell time, a moderate decrease of particles near the melt surface was observed, suggesting the onset of settling of particles. As melt was held for prolonged period of time (30 min and 45 min), upper part of the melt was decant due to progress of sedimentation. With these observations, the ability of QSM to save the spatial distribution of particles in the melt can be initially confirmed.

To quantify the visual observation, methods described in section 2.3 were employed. For samples taken from melt with 0 min, 15 min, 30 min and 45 min dwell time, the variation in ratio of area of particles to area of view field (RAA) due to sedimentation, plotted as a function of melt depth is shown in Figure 7. The RAA value of A356 – 17 vol.-% SiC is also given in the graph for reference. By using the average RAA value of "0 min" sample and RAA value of A356 – 17 vol.-% SiC, it can be calculated based on stereology principle that the particle volume fraction in the pre-prepared melt was 5.0 vol.-%. Given the discrepancy introduced by evaluating volume (3-D) via area (2-D), this value agrees with the 3.3 vol.-% particle volume fraction calculated from input material, which confirms a well-dispersed particle distribution in the melt under current stirring conditions. At 15 min dwell time, near the melt surface, a region with 2.5 mm – 10 mm depth was defined as an intermediate region since its RAA value was half of that of the lower region (A peak at 35 mm depth in the curve is temporarily ignored and will be discussed later). At 30 min dwell time, the presence of a distinct decant region with 2.5 mm – 23 mm depth was confirmed from the nearly unchanged 0 RAA value at the initial period of the curve. With the increase of depth, volume fraction of particles increased in a turbulent way and it was difficult to recognize again the intermediate region. When the melt was held for 45 min, the variation of particle volume fraction with the increase of depth resembled that of the "30 min" and the depth of decant region extended to 27.5 mm.

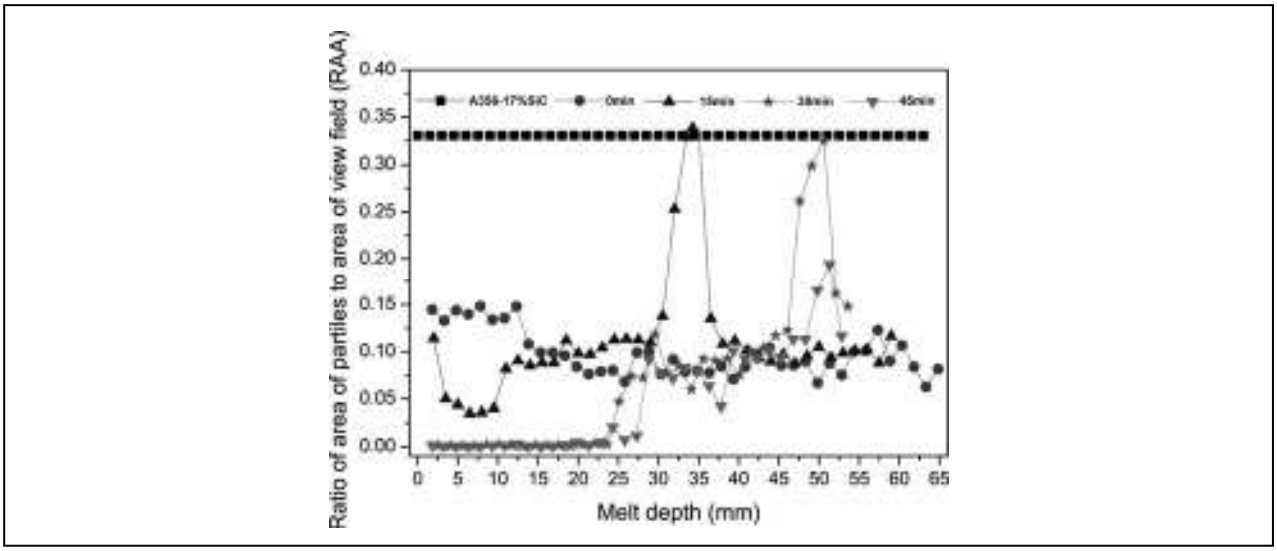

Figure 7: Variation of ratio of area of particles to area of view field with melt depth in samples taken from the melt with 0 min, 15 min, 30 min and 45 min dwell time.

Based on the difference in length of decant region, the moving velocity of clarification front, which is defined by the velocity at which the particles with the small size within the melt settles, is calculated to be around 0.005 mm/s. According to the modified Richardson and Zaki Equation [15], this settling velocity corresponds to that of a spherical particle with around 3 μm diameter, which is in concert with the size distribution particles in A356 – 17 vol. % SiC given in Figure 3(c) and therefore further confirm the ability of QSM to save the spatial distribution of particles in the melt.

As is readily noticed, in each of the curves of "15 min" and "45 min" sample, there is peak which indicates a nearly 17 vol.-% particle volume fraction at a certain depth. Take the "15 min" sample for example, micrograph taken at the position where peak arises (Figure 6 (a) and (c)) demonstrates that such a peak was a result of a presence of a large size "aggregate". It is speculated that such a kind of "aggregate" came from the sediments located at the very bottom of the melt in crucible (depth > 80 mm). The stirrer was not positioned deep enough to be able to disperse it. When the stirrer was drawn from the melt, a small amount of sediments attached to the stirrer and were brought to the upper part of the melt by disturbance. An interesting phenomenon worth noting is that the "aggregates" settled / suspended in the melt as an integral even at 30 min dwell time (Figure 6(a), near the bottom of "30 min column"), which indicates a strong electrostatic force between small clusters within the "aggregates".

3.3 Agglomeration

While applying QSM in current experimental procedure, particle information at the very bottom of the melt was lost, which precluded the possibility of correlating particle sedimentation with agglomeration in a quantitative way. Nevertheless, a rough impression of agglomeration of particles can be established by "observing" the microscopic distribution of particles at certain melt depth.

For samples taken from melt with 0 min, 15 min and 45 min dwell time, an OM micrograph was respectively taken at a region of 45 mm depth. Results are shown in Figure 8 together with a micrograph of A356-17 vol. % SiC.

Figure 8(a) shows the particle distribution in A356 – 17 vol.-% SiC. Apparently, particles with various sizes were well dispersed and clusters were hardly to find. At the end of stirring ("0 min" sample), clusters with size ranging from 50 to 80 μm were observed (Figure 8(b)). The formation of such clusters is ascribed to a moderate agglomeration of particles that occurs under current stirring conditions. Furthermore, it is speculated that particles with small size (less than 5 μm) contributed to the formation of these clusters as small pits were found in the contour of most clusters. As melt was held for prolonged period of time (15 min and 45 min), no obvious proceeding of agglomeration was found (Figure 8(c) and (d)), possibly suggesting a weak effect of sedimentation on agglomeration of particles.

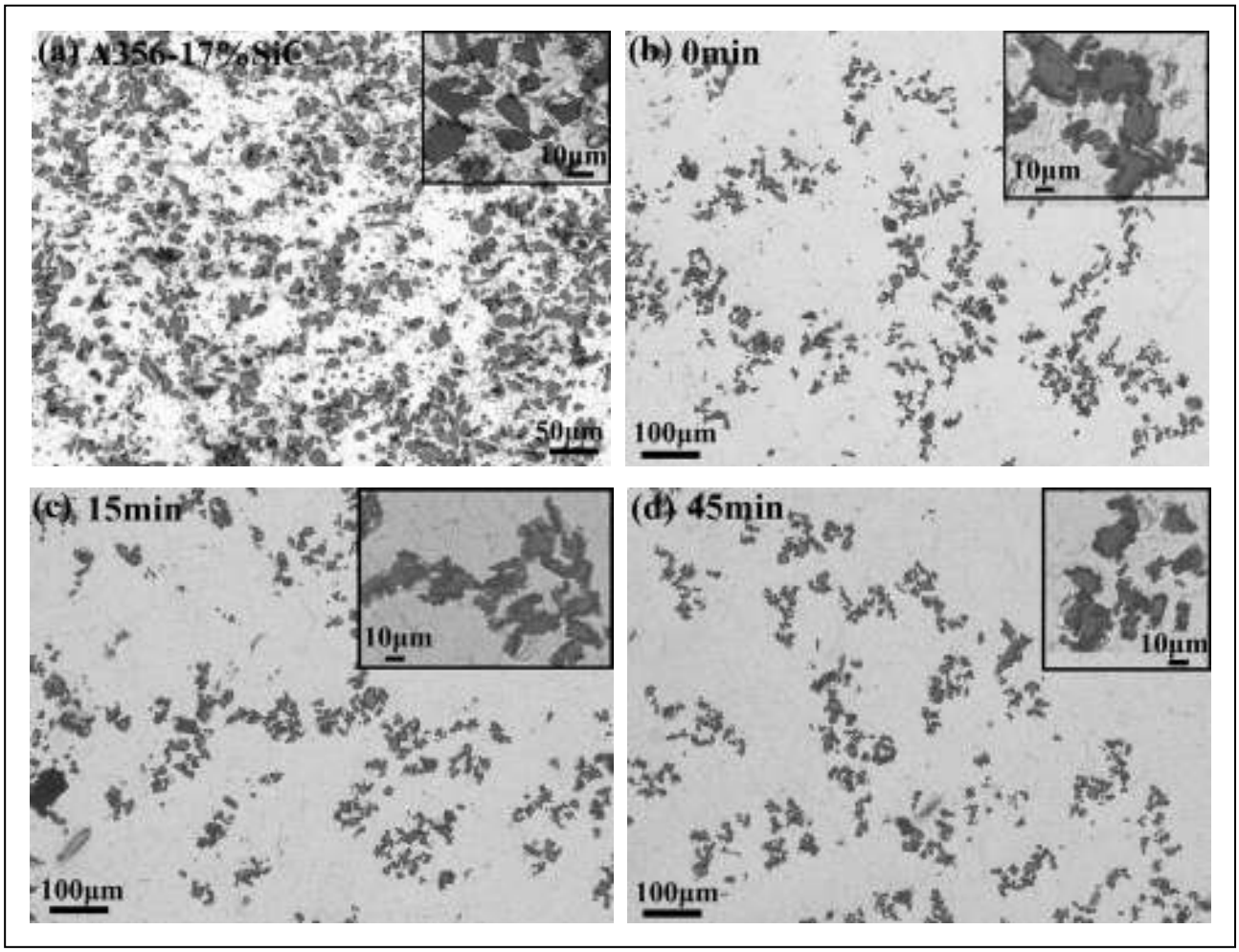

Figure 8: OM micrographs show distribution of SiC at the region of 45mm depth: (a) A356 – 17 vol.-% SiC; (b) – (d) samples taken from the melt with 0 min, 15 min and 45 min dwell time.

4 Conclusions

1. A quick sampling method (QSM) was developed to characterize the macroscopic and microscopic distribution of particles in the melt.
2. In a pre-prepared SiC particle-laden Al-Si melt, using QSM method:
   1) The sedimentation of particles was clearly observed. At 30 min and 45 min dwell time, a decant region were identified, based on which the moving velocity of clarification front were calculated to be 0.005 mm/s. This value agrees with that predicted by a modified Richardson and Zaki Equation.
   2) Agglomeration of SiC particles induced by stirring was illustrated.
3. In QSM sampling operation under current experimental procedures, around 20 wt. % loss is unavoidable. To alleviate this problem, a measure worth trying is to incorporate vacuum into QSM.

5 Acknowledgements

The research leading to these results was carried out in P4C (Project 4 Continuation) within AMAP (Advanced Metals and Processes Research Cluster, Project 4 Continuation) research cluster at RWTH Aachen University, Germany. Special thanks are addressed to China Scholarship Council (CSC) for the financial support of Cong Li.

6 References

[1] Surappa M.K. (2003): Aluminium matrix composites: challenges and opportunities - Sadhana, 28: 319 – 334.

[2] Li C., Li J., Mao Y., et al. (2017): Mechanism to remove oxide inclusions from molten aluminum by solid fluxes refining method - China Foundry, 14: 233 – 243.

[3] Hashim J., Looney L., Hashmi M.S.J. (2002): Particle distribution in cast metal matrix composites – Part I – Journal of Materials Processing Technology, 123: 251 – 257.

[4] Shorowordi K.M., Laoui T., Haseeb A., et al. (2003): Microstructure and interface characteristics of B_4C, SiC and Al_2O_3 reinforced Al matrix composites: a comparative study - Journal of Materials Processing Technology, 142: 738 – 743.

[5] Hashim J., Looney L., Hashmi M.S.J. (1999): Metal matrix composites: production by the stir casting method - Journal of Materials Processing Technology, 92: 1 – 7.

[6] Martin J.P., Dube G., Frayce D., et al. (2016): Settling phenomena in casting furnaces: a fundamental and experimental investigation – Essential Readings in Light Metals, Cham: 115-125.

[7] Sztur C., Balestreri F., Meyer J.L., et al. (2016): Settling of inclusions in holding furnaces: modeling and experimental results - Essential Readings in Light Metals, Cham: 107-114.

[8] Ravi K.R., Sreekumar V.M., Pillai R.M., et al. (2007): Optimization of mixing parameters through a water model for metal matrix composites synthesis – Materials & design, 28: 871 – 881.

[9] Gökelma M., Morscheiser J., Badowski M., et al. (2015): Observation on inclusion settling by LiMCA and PoDFA analysis in aluminium melts – International Aluminium Journal, 91: 56 – 61.

[10] Gökelma M., Latacz D., Friedrich B. (2016): A Review on Prerequisites of a Set-Up for Particle Detection by Ultrasonic Waves in Aluminium Melts – Open Journal of Metal, 6: 13.

[11] Doutre D.A., Guthrie R.I.L. (1985): Method and apparatus for the detection and measurement of particulates in molten metal – U.S. Patent, 4,555,662.

[12] Gökelma M., Le Brun P., Dang T., et al. (2016): Assessment of Settling Behavior of Particles with Different Shape Factors by LiMCA Data Analysis - Light Metals 2016. Springer, Cham: 843 – 848.

[13] Badowski M., Gökelma M., Morscheiser J., et al. (2015): Study of particle settling and sedimentation in a crucible furnace - Light Metals 2015. Springer, Cham: 967 – 972.

[14] Hanumanth G.S., Irons G.A., Lafreniere S. (1992) Particle sedimentation during processing of liquid metal-matrix composites. Metallurgical Transactions B, 23: 753 – 763.

[15] Irons G.A., Owusu-Boahen K. (1995): Settling and clustering of silicon carbide particles in aluminum metal matrix composites. Metallurgical and Materials Transactions B, 26: 981 – 989.

[16] Richardson J.F., Zaki W.N. (1954): Sedimentation and fluidization, Transactions of the Institution of Chemical Engineers, 32, 35 – 53.

[17] Zayan M.H., Jamjoom O.M., Razik N.A. (1990): High-temperature oxidation of Al-Mg alloys. Oxidation of Metals, 34: 323 – 333.

[18] Judge J.R., Vierbicky V.L. (1975): Sampling device for molten metal – U.S. Patent 3,915,014.

[19] Doutre D., Gariépy B., Martin J.P., et al. (2016): Aluminium cleanliness monitoring: methods and applications in process development and quality control - Essential Readings in Light Metals. Springer, Cham: 296 – 304.

[20] Instone S., Badowski M., Krings D. (2014): Sampling Tool for In-Depth Study of Furnace Processes - Light Metals 2014. Springer, Cham: 1003 – 1008.